Bulgarian Chemical Communications, Volume 56, Special Issue C (pp. 89-95) 2024 DOI: 10.34049/bcc.56.C.SI-20

Spectroscopic study on the solid-state structure of Pt(II) complexes of cycloalkanespiro-5-(2,4-dithiohydantoins)

A. Ahmedova [1*], P. Marinova [2], K. Paradowska [3], G. Tyuliev [4], M. Marinov [5], N. Stoyanov [6]

[1] *Faculty of Chemistry and Pharmacy, University of Sofia, 1, J. Bourchier Av., 1164 Sofia, Bulgaria*
[2] *Faculty of Chemistry, University of Plovdiv, 24, Tzar Assen Str., 4000 Plovdiv, Bulgaria*
[3] *Faculty of Pharmacy, Medical University of Warsaw, Banacha 1, 02097 Warsaw, Poland*
[4] *Institute of Catalysis, Bulgarian Academy of Sciences, 1113 Sofia, Bulgaria*
[5] *Agricultural University – Plovdiv, Department of Chemistry and Phytopharmacy, Faculty of Plant Protection and Agroecology, 12 "Mendeleev" Blvd, 4000 Plovdiv, Bulgaria;*
[6] *University of Ruse "Angel Kanchev" - Razgrad Branch, Department of Chemical, Food and Biotechnologies, 7200 Razgrad, 47 "Aprilsko Vastanie" Blvd., Bulgaria.*

Received: July 20, 2024; Revised: August 28, 2024

The molecular structure description of Pt(II) complexes of the bicyclic spiro-5-(2,4-dithiohydantoins) is a continuing challenge due to the large variety of coordination modes that the 2,4-dithiohydantoin heterocycle provides. Besides, the limited solubility of the complexes impedes the growth of good quality single crystals, which explains the lack of crystallographic data on metal complexes of spiro-5-(2,4-dithiohydantoins). The increasing interest on the biological activity of various Pt(II) complexes of 5-substituted 2,4-dithiohydantoins motivated the structural description we provide herein. This work describes a detailed analysis of the solid-state spectroscopic data on Pt(II) complexes of two cycloalkanespiro-5-(2,4-dithiohydantoins) bearing saturated and non-coordinating rings of seven or eight C-atoms. The experimental data from elemental analyses, FAB(+)-MS, XPS, IR and far-IR spectroscopies were used to model various structures of the complexes with the determined $M_2(L^-)_4$ composition. The solid state (CPMAS) ^{13}C NMR spectrum of the Pt(II) complex of cycloheptanespiro-5-(2,4-dithiohydantoin) was analyzed and its geometry was subjected to quantum chemical (Density Functional Theory, DFT) calculations with the B3LYP/6-31G(d,p)-(LanL2DZ; Pt) method. The coordination-induced changes in the calculated spectral characteristics (IR vibrations and ^{13}C NMR shifts) were compared with the experimentally measured ones for verification of the most plausible molecular structure of the complex. Based on the obtained results, a binuclear cubelike structure with two square planar Pt(II) centers holding the four ligand ions is suggested. In the best model structure, two of the N3-H deprotonated bridging ligands coordinate with their S2 thione atoms, whereas the other two ligands involve the S4 donor atoms in the coordination. The calculated Pt ⋯ Pt distance in the complex is 2.854 Å.

Keywords: cycloheptanespiro-5-(2,4-dithiohydantoin), cyclooctanespiro-5-(2,4-dithiohydantoin), platinum complexes, XPS, CPMAS NMR, GIAO DFT calculations

INTRODUCTION

The numerous biological activities of hydantoins, known initially for their use as antiepileptic drugs [1, 2], have recently been summarized in several review papers with the emphasis on their antileishmanial [3] or antimicrobial activity [4]. Earlier review papers highlight the broad spectrum of biological and pharmacological activities of hydantoin, thiohydantoin, and selenohydantoin compounds [5, 6]. Spiro-hydantoins, on the other hand, attracted attention with the noted aldosoreductase inhibition as a therapeutic approach to treat diabetes complication [7–9]. Ultimately, the anticancer activity of hydantoins, thiohydantoins [10–12], and spiro-hydantoins [13, 14] was extensively studied, which is further expanding to their metal complexes [15–20].

Our long-lasting interest on the coordination properties of cycloalkanespiro-5-(2,4-dithio hydantoins) started with the reported crystal structures of a series of derivatives with increasing number of C-atoms in the cycloalkane ring (5 to 8) [21]. Considering the highly conjugated dithio hydantoin ring which consists of two pairs of thioamide groups, the structural description of their metal complexes is a challenging spectroscopic task. Moreover, the only crystal structure of a dithiohydantoin metal complex is that of Cu(I) complex of 5,5-dimethyl-2,4-dithiohydantoin reported by Devillanova *et al.* in 1986 [22]. In our continuous attempts to make structural characterization of dithiohydantoin complexes we use combination of spectroscopic (^{13}C-CPMAS NMR, EPR, XPS, FAB-MS and IR) and quantum

* To whom all correspondence should be sent:
E-mail: *Ahmedova@chem.uni-sofia.bg*

chemical methods (DFT and GIAO DFT) to suggest the most plausible structures of the studied Cu(II) [23, 24], Pt(II) [20], Ni(II) and Cu(I) [25–27] complexes. In most cases we used ^{13}C-CPMAS NMR as the verification method for selecting the best theoretical model of the studied diamagnetic complexes.

In the present paper we describe the synthesis and characterization of Pt(II) complexes of two cycloalkanespiro-5-(2,4-dithiohydantoins), namely cycloheptanespiro-5-(2,4-dithiohydantoin) and cyclooctanespiro-5-(2,4-dithiohydantoin) denoted as **L1** and **L2**, respectively (Scheme 1). Several possible structures for the complexes were modeled accounting for the outlined general trends in the spectroscopic (^{13}C-CPMAS NMR and IR) changes seen for **L1** and **L2** after coordination with Cu(I) and Ni(II) ions that were earlier described [26].

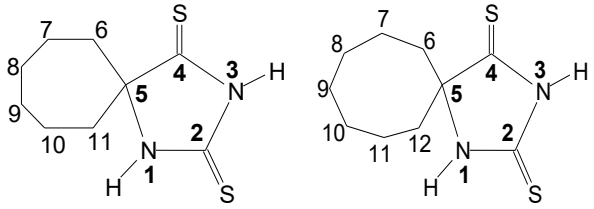

Scheme 1. Structural formulas of the studied ligands **L1** and **L2**.

EXPERIMENTAL

Methods and materials

All chemicals and solvents were analytical grade reagents and were used without purification. The *cis*-diamidodichloridoplatinum(II) (cisplatin) was purchased from Merck KGaA, Germany. Elemental analyses were performed on a Vario EU III instrument. The IR spectra were recorded in KBr pellets using a Nicolet 6700 Thermo-Scientific FT-IR spectrometer. FAR-IR spectra were recorded in CsI pellets on the same spectrometer equipped with DTGS polyethylene detector and far-IR solid-substrate beamsplitter. FAB(+)-MS spectra were obtained using a Fisons VG Autospec. ^{1}H- and ^{13}C-NMR spectra of the ligands were recorded on a Bruker DRX-250 spectrometer in DMSO-d_6. Solid-state cross polarization (CP) magic angle spinning (MAS) ^{13}C-NMR spectra were recorded on a Bruker Avance DSX-400 instrument at 100.61 MHz with high power proton decoupling; the samples were spun at 10 kHz in a 4 mm ZrO_2 rotor (contact time 2–9 ms, repetition time 30 s, 1024 scans). ^{13}C chemical shifts were calibrated indirectly through the glycine CO signal at 176.0 ppm relative to TMS. The photoelectron spectra (XPS) were measured at room temperature using an ESCALAB-MKII electron spectrometer (VG Scientific). The samples were pressed in pellets and the pressure in the UHV chamber was 5×10^{-9} mbar during the measurements. The MgKa radiation (1253.6 eV) was used for the excitation. The instrumental resolution was ~ 1.0 eV as measured by the fullwidth at half maximum (FWHM) of the $Ag3d_{5/2}$ photoelectron line. The accuracy of binding energy (EB) determination is ± 0.1 eV. The 285.0 eV of C1s peak was used as an energy reference.

Synthesis and characterizations

The ligands **L1** and **L2** were synthesized according to a previously described procedure [28]. The products were recrystallized from methanol/water solution and characterized with melting point, elemental analyses, IR and NMR spectra in solution and in solid state. The analytical data of the ligands agree with the published ones [28].

The Pt(II) complexes of **L1** and **L2** were obtained by mixing 20 mL of water solution of 0.1 mmol (30 mg) cisplatin and 0.2 mmol of the ligands (43 mg of **L1** and 45 mg of **L2**) dissolved in 20 mL of THF. The reaction mixtures were stirred at room temperature for 48 h, leading to the formation of yellow-greenish precipitates, which were filtered off, dried at 45 °C overnight, and stored in a desiccator under P_2O_5.

Complex **Pt-L1**: Yield 36 mg (53.3% based on platinum); M.p. > 350 °C; FAB(+)-MS: $[M\text{-}H]^+$ 1243.3 m/z (*20*), $Pt_2(\mathbf{L1}^-)_4$ MW=1242.1. IR (KBr): ν (cm^{-1}) 3400 br (H_2O), 3190 s, br (NH), 2928 vs, 2856 s (CH_2), 1718 w, 1628 w, 1560 vs, 1496 vs, 1457 vs, 1411 s, 1355 s, 1328 vs, 1279 s, 1244 s, 1183 vs, 1115 vs, 983 w, 943 w, 843 w, 621 w, 575 w, 464 w, 432 w; IR (CsI): ν (cm^{-1}) 390 m, 370-364 w, 338 w, 305 w, 273 w, 229 s br; Calcd for $Pt_2(\mathbf{L1}^-)_4\times6H_2O$ ($C_{36}H_{64}N_8O_6Pt_2S_8$, MW=1351.59): C 31.99%; H 4.77%; N 8.29%; S 18.98%; found: C 31.84%; H 4.66%; N 8.98%; S 18.95%.

Complex **Pt-L2**: Yield 47 mg (66.7% based on platinum); M.p. > 350 °C; FAB(+)-MS: $[M\text{-}H]^+$ 1300.3 m/z $Pt_2(\mathbf{L2}^-)_4$ MW=1298.2. IR (KBr): ν (cm^{-1}): 3400 br, 3188 m(NH), 2923 vs, 2852 s (CH_2), 1720-1626 w, 1558 s, 1498 vs, 1470 vs, 1410 s, 1351 vs, 1327 vs, 1264 s, 1201 s, 1158 vs, 1117 s, 1092 s, 980 w, 937 w, 842 w, 807 w, 763 w, 678 w, 496-468 w, 441 w; IR (CsI): ν (cm^{-1}) 338 sh, 292 w br, 257 m br, 207 m br; Calcd for $Pt_2(\mathbf{L2}^-)_4\times6H_2O$ ($C_{40}H_{72}N_8O_6Pt_2S_8$, MW=1407.73): C 34.13%, H 5.16%, N 7.96%, S 18.22%; found: C 34.11%; H 4.93%; N 8.77%; S 18.27%.

The vibrational frequencies of the free ligands are given to facilitate the discussion of their coordination modes. **L1**: IR (KBr): ν (cm^{-1}): 3145 vs (NH), 2933 m (CH_2), 2845 m (CH_2), 1541 vs, 1426 vs, 1348 m, 1260 m, 1231 s, 1159 s, 1126 s, 1107 m, 1045 m, 890 w, 841 m, 730 w, 688 m, 582 w, 527 m, 463 m, 441 w; Far-IR (CsI): ν (cm^{-1}): 352 sharp, 330 sharp, 288 s , 274 s, 220 w, 199 s sharp, 155 w; **L2**: IR (KBr): ν (cm^{-1}): 3160 s (NH), 2939 s, 2856 m (CH_2), 1540 vs, 1438 m, 1427 vs, 1260 s, 1210 s, 1145 s, 1107 vs, 1063 w, 929 m, 735 w, 710 m, 626 m, 542 m, 453m; Far-IR (CsI): ν (cm^{-1}): 381 sharp, 309 sharp, 268 s, 248 w, 220 sharp, 202 sharp, 126 s.

Quantum chemical calculations

Geometry optimizations of **L1** and its Pt(II) complex, **Pt-L1**, were performed using the DFT method with the hybrid B3LYP functional [29, 30] as implemented in the Gaussian 09 software [31]. A mixed basis set, double-ζ Pople-type 6-31G(d,p) for all light elements and Los Alamos National Laboratory 2 double-ζ basis set (LANL2DZ) for platinum, was used. Harmonic vibrational frequencies and intensities were computed at the same level of theory for **L1** and **Pt-L1** and convergence to local minima was confirmed. The NMR shielding constants were calculated using the gauge-including atomic orbitals, GIAO-DFT, method [32] and the calculated isotropic ^{13}C-NMR shielding constants, σ_i, were converted to ^{13}C chemical shifts using the equation: $\delta_i = 191.818 - \sigma_i$.

RESULTS AND DISCUSSION

The Pt(II) complexes were isolated as yellow-greenish powders and their composition was derived from elemental analyses and FAB(+)-MS measurements. The data indicated on $Pt_2(L^-)_4$ molecular composition formed with coordination of deprotonated ligand anions (L^-). Theoretically calculated isotopic distribution for the molecular ion peak with the suggested composition is compared with the experimentally obtained one for **Pt-L1** in Figure 1. The virtually same pattern confirms the presence of two platinum centers in the registered peak of the molecular ion. Similar data are seen for the **Pt-L2** complex.

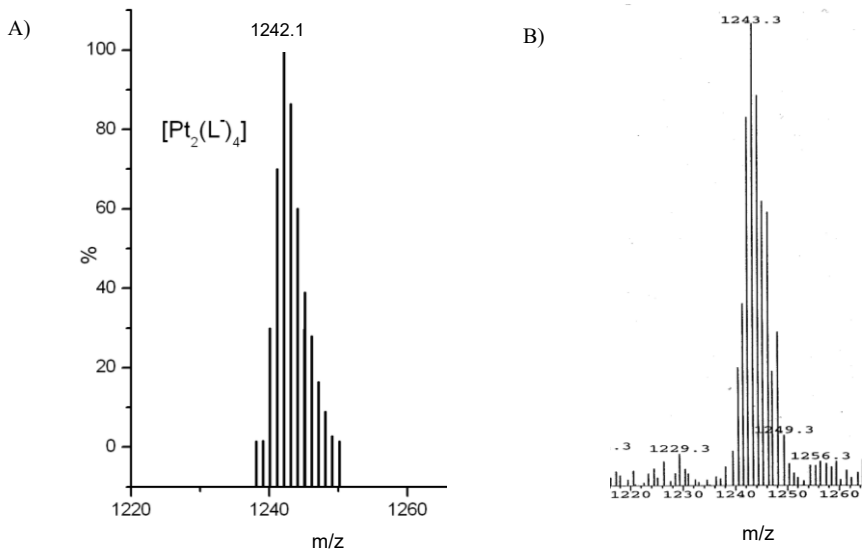

Figure 1. Comparison of **A**) the calculated isotopic distribution pattern of the molecular composition $Pt_2(\mathbf{L1}^-)_4$ (MW=1242.1) with **B**) the experimental FAB(+)-MS spectrum of **Pt-L1** (molecular ion peak $[M-H]^+$ 1243.3).

Table 1. Binding energies (E_B) in eV of C1s, N1s, S2p and Pt4f electrons in the studied ligands **L1** and **L2** and their Pt(II) complexes, **Pt-L1** and **Pt-L2**.

Compounds / Electron shell	**L1**	**Pt-L1**	**L2**	**Pt-L2**
C1s	285.0	285.0	285.0	285.0
N1s	400.6	400.2	400.6	400.2
$S2p_{3/2}$	162.8	163.2	162.7	163.1
$Pt4f_{7/2}$	–	73.0	–	73.0

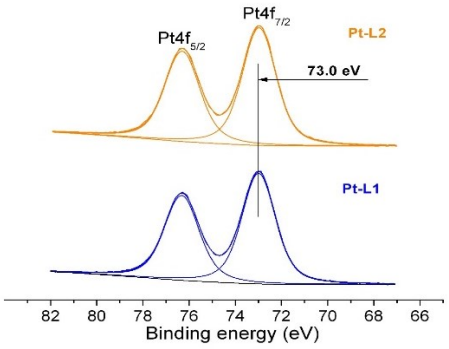

Figure 2. X-ray photoelectron spectra (XPS) of the Pt4f electrons of the **Pt-L1** and **Pt-L2** complexes.

To conclude whether both platinum centers in the complex are distinguishable we performed XPS measurements of the free ligands and the corresponding complexes. Data are summarized in Table 1 and the regions of the XPS spectra for the Pt4f-electrons binding energies are depicted in Figure 2. From Figure 2 it can be seen that for both Pt(II) complexes only the expected two peaks for the 4f–electrons of Pt(II), split by the spin-orbit coupling to $Pt4f_{5/2}$ and $Pt4f_{7/2}$ in the 3:4 ratio, are present. This could suggest that both platinum centers in the complex are surrounded by the coordinated ligands in an identical way. Rather symmetrical Lorentzian line shape for the $Pt4f_{7/2}$ electrons is registered with virtually the same energy, 73.0 eV for both **Pt-L1** and **Pt-L2**. Similar values of the binding energies are reported for other Pt(II) complexes coordinated in bidentate way with thiourea derivatives [33]. The data in Table 1 show that the binding energies of N1s and $S2p_{3/2}$ electrons change upon coordination in opposite directions – a decrease for N1s electrons by 0.4 eV and increase of the $S2p_{3/2}$ binding energies of 0.4 is observed for both complexes. These observations are consistent with the proposed deprotonation of one of the NH groups and coordinated thione sulfur atom through dative bond formation with Pt(II).

As both complexes, **Pt-L1** and **Pt-L2**, showed limited solubility in most solvents, we could study their structure only in the solid state by means of IR and CPMAS NMR spectroscopy, since no single crystals could be grown for crystallographic analysis. The experimental evidence for coordination of deprotonated ligands **L1** and **L2** was derived from the observed changes in their IR spectra. The general trends in the IR spectra of the complexes can be summarized as follows: i) shift of the characteristic N-H stretching of the free ligands (centered at 3145 and 3160 cm^{-1} of **L1** and **L2**) to 3190 and 3188 cm^{-1} in the spectra of **Pt-L1** and **Pt-L2**, respectively; ii) strong shifts and splitting for the most intense vibrations of the thioamide groups at 1541 and 1540 cm^{-1} of **L1** and **L2**, which appear at 1560, 1496 and 1558, 1498 cm^{-1} in the complexes **Pt-L1** and **Pt-L2**, respectively; iii) similar trend for the other set of thioamide vibrations at 1426 and 1438 cm^{-1} of **L1** and **L2**, which appear at 1457, 1411 and 1470, 1410 cm^{-1} in the complexes **Pt-L1** and **Pt-L2**, respectively; iv) red shift of the free ligands' vibrations at 1260 and 1159 cm^{-1} to 1279 and 1183 cm^{-1} upon coordination in **Pt-L1**, and similarly for the bands at 1260 and 1145 cm^{-1} shifting to 1264 and 1158 cm^{-1} in **Pt-L2**. These changes after coordination to Pt(II) can be explained with the presumed bridging coordination by one thione sulfur atom and a deprotonated amine nitrogen. It should be noted, however, that the complex nature of the highly conjugated dithiohydantoin ring, consisting of two thioamide pairs, makes it impossible to distinguish between the many other possible coordination modes. The far-IR spectra were used to examine the vibrational frequencies involving the coordinated Pt(II) ion. In the spectrum of **Pt-L1** broad vibrations appear at 390, 273 and 229 cm^{-1} and weak bands in the region 370–364–338 and 305 cm^{-1}. Similarly, these are seen at 338, 292, and 257 cm^{-1} in the **Pt-L2** spectrum.

Bridging mode of coordination has been earlier suggested for Pt(II) complexes of other dithiohydantoin ligands with bulky substituent at the spiro-C5 atom [20]. Considering their structural similarity with the ligands **L1** and **L2** studied herein, we applied quantum chemical methods to verify the most plausible structure expected for the **Pt-L1** complex. Geometry optimizations with DFT B3LYP/6-31G(d,p)/(LANL2DZ; Pt) method were performed on three model structures for **Pt-L1** (Scheme 2), assuming $M_2(L^-)_4$ composition and bridging coordination of deprotonated N3-H group of the ligand **L1**. For each optimized structure the corresponding spectroscopic characteristics – vibrational (IR) frequencies and nuclear magnetic shielding – were calculated and compared with the available experimental data to select the best theoretical model for the structure of **Pt-L1**.

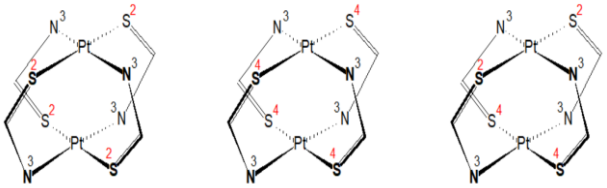

Scheme 2. Schematic presentation of the structural variations of the cubelike geometry of the optimized models for **Pt-L1** complex. From left to right: all N3^S2 bridging ligands; all N3^S4 bridging ligands; mixed two N3^S2 and two N3^S4 bridging ligands.

The reason to model three combinations of coordinated bridging ligands is to try to find explanations of the observed ^{13}C-CPMAS NMR spectrum of **Pt-L1** which is compared with that of **L1** in Figure 3. The measured ^{13}C chemical shifts are listed in Table 2. All three C-atoms from the dithiohydantoin ring (C2, C4 and C5) exhibit downfield shift after coordination, which is estimated to 7.5 ppm for C2 and to 3.8 ppm for C5. The signal of C4 atom exhibits splitting of 16 ppm in the spectrum of **Pt-L1**. That is why we modeled also mixed type of coordination of the ligands except the models with all N3^S2 and all N3^S4 bridging ligands (Scheme 2). An acceptable result was obtained with the assumed N3^S2 - N3^S4 mixed type of coordination of the four ligand ions in the dimeric **Pt-L1** complex. The calculated shifts for C4 atoms in **Pt-L1** differ by *ca.* 7 ppm (220.1 / 213.3, see Table 2), whereas the signals for C2 differ by 2 ppm (185.3 / 183.3). Considering the resolution of the ^{13}C-CPMAS NMR spectra of amorphous samples and their larger half-widths, we proposed as the best model structure for the **Pt-L1** complex the one with mixed type N3^S2 - N3^S4 bridging coordination.

The optimized (B3LYP/6-31G(d,p)/LanL2DZP) structure of the **Pt-L1** complex, with the mixed type of N3^S2 - N3^S4 bridging coordination, is depicted in Figure 4. The Pt ⋯ Pt distance in the complex is 2.854 Å, whereas the Pt-N and Pt-S bond lengths are 2.06 Å and 2.40 Å, respectively. It should be noted that the non-coordinated sulfur atoms in the complexes are able to form additionally either intermolecular hydrogen bonding or even coordination with other Pt(II) centers. In the latter case polymeric structure of the complexes can be realized, which would explain their low solubility.

Similar cubelike structure of a Pt(II) complex has been characterized by single-crystal X-ray analyses on dimeric Pt(II) complexes of tetrazole thiol ligand with bridging N^S coordination [34]. The experimentally measured Pt ⋯ Pt distance is 2.8190(5) Å, which is shorter than the calculated one for the studied **Pt-L1** complex.

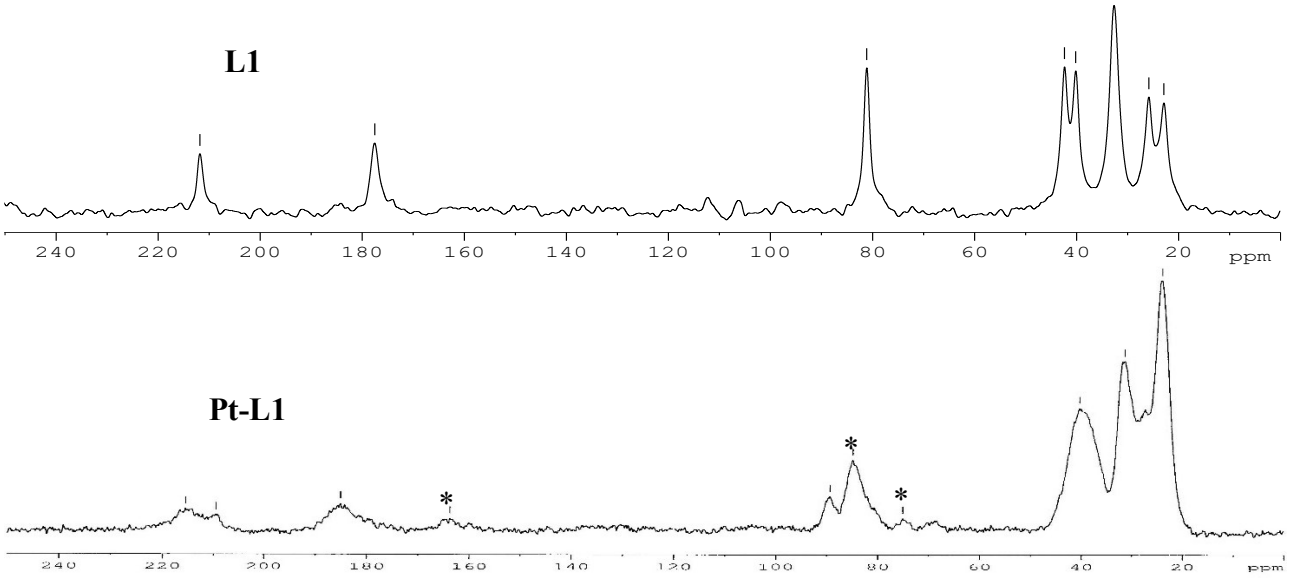

Figure 3. ^{13}C-CPMAS NMR spectra of the free ligand **L1** (top) and its complex **Pt-L1**. Asterisks denote the spinning side bands.

Table 2. ^{13}C NMR data for **L1** and its Pt(II) complex **Pt-L1**. The ^{13}C CPMAS chemical shifts are given in bold and compared with the calculated ones (GIAO-B3LYP/6-31G(d,p)//B3LYP/6-31G(d,p)). For atoms numbering see Scheme 1. The values in brackets relate to the C-atoms from the second N3^S4 bridging ligand, and the asterisks denote the values of the C-atoms from the N3^S4 bridging ligands.

	Ligand L1		Pt-complex of L1	
Atom number	**CPMAS**	B3LYP	**CPMAS**	B3LYP
C2	**177.6**	174.21	**185.1**	186.03 (185.31) / 183.28*
C4	**211.8**	209.22	**215.6 / 209.6**	220.14 (219.64) / 213.3*
C5	**81.1**	79.84	**84.9**	78.96 / 78.71*
C6	**40.2**	43.09	**40.3**	44.26 / 43.30*
C7	**22.9**	24.46	**23.7**	24.05 / 23.14*
C8	**32.7**	33.72	**31.2**	33.66
C9	**32.7**	32.83	**31.2**	32.24
C10	**25.9**	26.46	**24.1**	26.45 / 25.04*
C11	**42.4**	43.47	**40.3**	42.24 / 41.74*

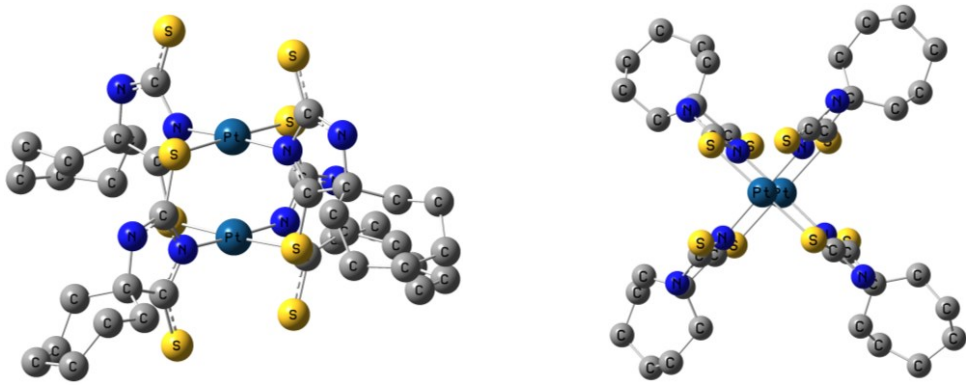

Figure 4. Optimized structure of **Pt-L1** with composition $Pt_2(L^-)_4$ and bridging coordination of deprotonated ligand: (left) side view; (right) top view. Hydrogen atoms are omitted for clarity.

CONCLUSIONS

In this work we addressed the challenging task of structural description of the Pt(II) complexes of two cycloalkanespiro-5-(2,4-dithiohydantoins) with either seven or eight C-atoms in the saturated non-coordinating ring (**L1** and **L2**). Both complexes were obtained using cisplatin as starting platinum(II) salt with the aim to isolate its analogue. The chemical analysis and FAB(+)-MS data indicated, however, that all ligands in the starting salt are replaced by the studied 2,4-dithiohydantoins and the formed complexes have a $M_2(L^-)_4$ composition. Further supported by the XPS, IR and far-IR measurement we presumed a bridging coordination of deprotonated N3-H group of the ligands for both complexes with binuclear cubelike structure with two square planar Pt(II) centers holding the four ligands. The solid state (CPMAS) ^{13}C NMR spectrum of the Pt(II) complex of cycloheptanespiro-5-(2,4-dithiohydantoin), **Pt-L1**, was used as a verification tool to select the most plausible model structures that were modeled and optimized by quantum chemical (DFT) calculations. Direct comparison of the coordination-induced changes in the experimentally measured and the calculated spectral characteristics (IR vibrations and ^{13}C NMR shifts) from the (GIAO-) B3LYP/6-31G(d,p)-(LanL2DZ; Pt) calculations allowed us to suggest the best model structure for **Pt-L1**, in which two of the N3-H deprotonated bridging ligands coordinate with their S2 thione atoms, whereas the other two ligands involve the S4 donor atoms in the coordination.

Although the initial motivation of our research was driven by the biological potential of the studied ligands and their Pt(II) complexes, it should be noted that the structural aspects of the formed metal complexes deserve special attention, too. The highly diverse coordination modes of the 2,4-dithiohydantoins, although challenging from spectroscopic viewpoint, offer a rich supramolecular landscape that may open other areas of potential application of their metal complexes. Proper selection of starting salts and synthetic conditions for obtaining good quality single crystals for crystallographic analyses poses as a future perspective of high value.

Acknowledgement: The Bulgarian National Center for High performance and Distributed Computing (The National Roadmap for Research Infrastructures: 2018-2023) through its facilities in Sofia University (PhysON cluster, NIS-3318) is gratefully acknowledged for the provided access to computational resources.

REFERENCES

1. D. Janz, *Der Nervenarzt*, **21,** 113 (1950).
2. F. Broser, *Nervenarzt*, **37**, 25 (1966).
3. T. Mahender, W. Pankaj, S. P. Kumar, V. Ankur, S. S. Kumar, *Mini-Rev. in Med. Chem.,* **22**, 743 (2022).
4. M. K. Langer, A. Rahman, H. Dey, T. Anderssen, H. M. Blencke, T. Haug, K. Stensvåg, M. B. Strøm, A. Bayer, *Eur. J. Med. Chem.*, **249** , 115147 (2023).
5. S. Cho, S.-H. Kim, D. Shin, *Eur. J. Med. Chem*., **164**, 517 (2019).
6. Z. Moussa, M. A. M. Sh. El-Sharief, S. Y. Abbas, *Eur. J. Med. Chem.*, **122**, 419 (2016).
7. R. Sarges, R.C. Schnur, J.L. Belletire, M.J. Peterson, *J. Med. Chem.,* **31**, 230 (1988).
8. Z. Y. Jiang, Z. Qiong-Lin, J. W. Eaton, W. H. Koppenol, J. V. Hunt, S. P. Wolff, *Biochem. Pharmacol.,* **42**, 1273 (1991).
9. L. Somsak, V. Nagy, Z. Hadady, T. Docsa, P. Gergely, *Curr. Pharm. Design*, **9**, 1177 (2003).
10. A. M. Al-Obaid, H. I. El-Subbagh, A. Khodair, M. M. A. Elmazar, *Anti-Cancer Drugs*, **7**, 873 (1996).
11. Y. Liu, J. Wu, P.-Y. Ho, L.-C. Chen, C.-T. Chen, Y.-C. Liang, C.-K. Cheng, W.-S. Lee, *Cancer Lett.,* **271**, 294 (2008).
12. P. Marinova, M. Marinov, M. Kazakova, Y. Feodorova, D. Blazheva, A. Slavchev, H. Sbirkova-Dimitrova, V. Sarafian, N. Stoyanov, *Russ. J. Gen. Chem*., **91**, 939 (2021).

13. C. S. A. Kumar, S. B. B. Prasad, K. Vinaya, S. Chandrappa, N. R. Thimmegowda, S. R. Ranganatha, S. Swarup, K. S. Rangappa, *Inv. New Drugs*, **27**, 131 (2009).
14. C. V. Kavitha, M. Nambiar, C. S. Ananda Kumar, B. Choudhary, K. Muniyappa, K. S, Rangappa, S. C. Raghavan, *Biochem. Pharmacol.*, **77**, 348 (2009).
15. A. Bakalova, R. Buyukliev, R. Nikolova, B. Shivachev, R. Mihaylova, S. Konstantinov, *Anti-Cancer Agents in Med. Chem*., **19**, 1243 (2019).
16. P. E. Marinova, M. N. Marinov, M. H. Kazakova, Y. N. Feodorova, V. S. Sarafian, N. M. Stoyanov, *Bulg. Chem. Commun*., **47** (Spec. Iss. A), 75 (2015).
17. P. Marinova, M. Marinov, M. Kazakova, Y. Feodorova, P. Penchev, V. Sarafian, N. Stoyanov, *Biotech. & Biotech. Equip.,* **28**, 316 (2014).
18. A. Bakalova, R. Buyukliev, H. Varbanov, G. Momekov, *Inorg. Chim. Acta*, **423**, 46 (2014).
19. A. Bakalova, H. Varbanov, R. Buyukliev, G. Momekov, D. Ferdinandov, S. Konstantinov, D. Ivanov, *Eur. J. Med. Chem.*, **43**, 958 (2008).
20. A. Ahmedova, G. Pavlović, M. Marinov, P. Marinova, G. Momekov, K. Paradowska, S. Yordanova, S. Stoyanov, N. Vassilev, N. Stoyanov, *Inorg. Chim. Acta*, **528**, 120605 (2021).
21. B. Shivachev, R. Petrova, P. Marinova, N. Stoyanov, A. Ahmedova, M. Mitewa, *Acta Cryst. Sect. C: Cryst. Struct. Commun.,* **62**, o211 (2006).
22. F.A. Devillanova, A. Diaz, F. Isaia, G. Verani, L. P. Battaglia, A. B. Corradi, *J. Coord. Chem.*, **15**, 161 (1986).
23. A. Ahmedova, P. Marinova, M. Marinov, N. Stoyanov, *J. Mol. Struct.*, **1108**, 602 (2016).
24. A. Ahmedova, P. Marinova, K. Paradowska, M. Marinov, M. Mitewa, *J. Mol. Struct.,* **892**, 13 (2008).
25. A. Ahmedova, P. Marinova, K. Paradowska, N. Stoyanov, I. Wawer, M. Mitewa, *Inorg. Chim. Acta*, **363**, 3919 (2010).
26. A. Ahmedova, P. Marinova, K. Paradowska, M. Marinov, I. Wawer, M. Mitewa, *Polyhedron*, **29**, 1639 (2010).
27. A. Ahmedova, P. Marinova, G. Tyuliev, M. Mitewa, *Inorg. Chem. Commun*., **11**, 545 (2008).
28. M. Marinov, S. Minchev, N. Stoyanov, G. Ivanova, M. Spassova, V. Enchev, *Croat. Chem. Acta,* **78**, 9 (2005).
29. S. Lee, W. Yang, R. G. Parr, *Phys. Rev. B*, **37**, 785 (1998).
30. A. D. Becke, *J. Chem. Phys*., **98**, 5648 (1993).
31. M. J. Frisch, G. W. Trucks, D. J. Fox, et al. Gaussian 09, Revision A.02, Gaussian, Inc., Wallingford CT, 2009.
32. J. R. Cheeseman, G. W. Trucks, T. A. Keith, M. J. Frisch, *J. Chem. Phys.*, **104**, 5497 (1996).
33. W. Hernández, E. Spodine, R. Richter, K. H. Hallmeier, U. Schröder, L. Beyer, *Zeitschr. Anorg. Allgem. Chem.*, **629**, 2559 (2003).
34. M. S Majdolashrafi, A. Raissi Shabari, V. Amani, *Phosphorus, Sulfur, and Silicon, and the Related Elements*, **192**, 1188 (2017).